Theory of orientation-sensitive near-edge fine-structure core-level spectroscopy

M. Nelhiebel
LMSS-Mat, CNRS-UMR 8579, École Centrale Paris, F-92295 Châtenay-Malabry, France

P.-H. Louf and P. Schattschneider
Institut für Angewandte und Technische Physik, Technische Universität Wien, A-1040 Vienna, Austria

P. Blaha and K. Schwarz
Institut für Physikalische und Theoretische Chemie, Technische Universität Wien, A-1060 Vienna, Austria

B. Jouffrey
LMSS-Mat, CNRS-UMR 8579, École Centrale Paris, F-92295 Châtenay-Malabry, France

(Received 16 November 1998)

We derive an expression for the double differential scattering cross section for inner-shell excitation of atoms by fast electrons. Using the augmented plane-waves approach for description of the photo electron, we find the inelastic scattering cross section to be a function of energy loss and momentum transfer, which is *a priori* not proportional to the local symmetry-projected unoccupied density of states. We show the importance of symmetries and choice of coordinate systems, which may necessitate the consideration of cross terms in the expression for the inelastic scattering cross section, coupling different angular momenta of the final state. This has important consequences for the interpretation of energy loss near-edge structure and its counterpart x-ray absorption near edge structure. [S0163-1829(99)00820-6]

I. INTRODUCTION

The double differential scattering cross section for the excitation of an atom by a fast electron is given in the first Born approximation by[1]

$$\frac{\partial^2\sigma}{\partial E\,\partial\Omega}=\frac{4\gamma^2}{a_0^2}\frac{k}{k_0}\frac{1}{Q^4}S(\mathbf{Q},E), \tag{1}$$

where we defined the dynamic form factor (DFF)

$$S(\mathbf{Q},E)=\sum_{i,f}\left|\langle i|e^{i\mathbf{QR}}|f\rangle\right|^2\delta(E+E_i-E_f). \tag{2}$$

a_0 is the Bohr radius, $\gamma=(1-\beta^2)^{-1/2}$ the relativistic factor, and k_0,k the length of the fast electron's wave vectors $\mathbf{k}_0$ and $\mathbf{k}$ before and after interaction, respectively. The kinematics of scattering define $\mathbf{Q}=\mathbf{k}_0-\mathbf{k}$, the scattering vector in the Fourier-transformed Coulomb interaction potential. In the case where the dipole approximation $e^{i\mathbf{QR}}\simeq 1+i\mathbf{QR}$ is justified, the direction of $\mathbf{Q}$ plays the same role as the polarization vector $\boldsymbol{\epsilon}$ does in x-ray absorption spectrometry (XAS) for moderate photon energies, and formulas derived for electron energy loss spectrometry (EELS) may be applied to XAS.[2,3]

The DFF is essentially a sum, restricted by conservation of energy $E_f-E_i=E$ with E the energy transferred from the fast electron to the atom, over transition probabilities between initial and final eigenstates belonging to the atom's Hamiltonian. In the one-electron approximation these states are one-particle wave functions.

In order to explain observed edge shapes in EELS, the DFF in Eq. (2) was repeatedly evaluated, in the past for isolated atoms,[4,5] more recently for atoms embedded in the potential created by neighboring atoms (e.g., Refs. 3, 6, 7, and references therein). As already argued in the beginning of EELS,[8,9] the detailed fine structure of an edge is due to the influence of the crystal potential on the final state $|f\rangle$, and thus the observed electron loss near-edge structure (ELNES) might be explained by referring to the unoccupied density of states (DOS).

Modern methods[10] for a simulation of ELNES employ density-functional theory (DFT) combined with an adequate expression for the exchange and correlation potential[11] as a tool to obtain single-electron wave functions for the final state. Often, the dipole approximation is used and integration over all directions of scattering is implied. A major advantage of EELS, namely the ability of selecting $\mathbf{Q}$, is thus deliberately wasted, and indeed interpretation of momentum resolved ELNES is rare and mostly qualitative,[2,12,13] even though its principal interest is generally admitted.

On the other hand, the experimentalist is confronted with an ambiguous definition of the transition-matrix element. In real-space (multiple scattering) methods[14,15] the matrix element in Eq. (2) is explicitly evaluated, taking into account reflection of the photoelectron wave function by neighboring atoms, and is traced back to an expression proportional to the unoccupied DOS.[16,17] In reciprocal-space band-structure methods the transition-matrix element is *a priori* taken as a mere weighting factor to the DOS $\chi(E)$,

$$S(Q,E)=|M(Q,E)|^2\chi(E). \tag{3}$$

As a formal justification of Eq. (3), Fermi's golden rule is employed.[18] In practice, the dipole-selection rule is ''superimposed'' on Eq. (3) to yield

$$S(Q,E)=[|M_{l+1}(Q,E)|^2\chi_{l+1}(E) + |M_{l-1}(Q,E)|^2\chi_{l-1}(E)], \quad (4)$$

where l is the angular-momentum quantum number of the initial state. Often, the energy dependence of the matrix elements $|M_{l\pm1}(Q,E)|^2$ is neglected and the ELNES is directly compared to the partial DOS.

We show that the formulation of Eq. (3) is somewhat arbitrary, and derive the DFF by an explicit evaluation of the matrix element squared in Eq. (2), using a band-structure approach in reciprocal space. This may indeed lead to the partial DOS under the restriction that one takes an average over all directions of **Q**. This condition is mentioned in the original works[19,20] to which most authors refer when they compare ELNES to the partial DOS, but it often passes unnoticed afterwards. In the case where **Q** has a definite direction and no integration is performed, we show that the DOS may be insufficient to describe the ELNES, and the more complex expression of Eq. (12) must be used, involving various eigenstates to the angular momentum of the final state.

II. A FORMULA FOR (Q,*E*) RESOLVED ELNES

We study the inner-shell excitation of a given atom surrounded by other atoms, in the special geometry defined by the crystal. As we shall see, the calculation proceeds along the same lines as for single isolated atoms.[4,5] We use for the initial (core) state of energy $E_{n,l}$ an atomic wave function separable into a radial and an angular part

$$\langle \mathbf{R}|i\rangle = u_{nl}(R)Y_m^l(\tilde{\mathbf{R}}) \quad (5)$$

with $\tilde{\mathbf{R}}=\mathbf{R}/R$, and expand the interaction operator into spherical waves,

$$e^{i\mathbf{QR}}=4\pi\sum_{\lambda=0}^{\infty}\sum_{\mu=-\lambda}^{+\lambda} i^\lambda Y_\mu^\lambda(\tilde{\mathbf{Q}})^* Y_\mu^\lambda(\tilde{\mathbf{R}})j_\lambda(QR), \quad (6)$$

where $j_\lambda(x)$ is the spherical Bessel function of order λ. The core-level state $|i\rangle$ is supposed to be completely sharp in energy, and we assume that contributions from different n,l are sufficiently separated in energy so that we have only to sum over degeneracy m, as well as the two magnetic-spin quantum numbers.

The sum over final eigenstates to the one-particle Hamiltonian in the crystal is a sum over band indices ν and wave vectors $\mathbf{k}$ in the first Brillouin zone, determining a Bloch state $|\nu\mathbf{k}\rangle$ of energy $E_{\nu\mathbf{k}}$. As the initial state wave function decays very rapidly with increasing R, we can consider the matrix elements in Eq. (2) to be nonvanishing only inside of a sphere of radius R_t centered on atom t. This is the reason why ELNES is said to test the *local* DOS. We, thus, need an expression for the band state $|\nu\mathbf{k}\rangle$ only inside this sphere. Among the many different methods to obtain one-particle Bloch states for electrons in crystals, we choose Slater's augmented plane-wave method since it intrinsically is based on an expansion of the Bloch state into atomlike waves inside of spheres centered on the atoms, matched to plane waves in the interstitial region.[21] The band state's component inside of sphere t reads

$$\psi_{\nu\mathbf{k}}^t(\mathbf{R})=\sum_{l'=0}^{\infty}\sum_{m'=-l'}^{+l'} D_{l'm'}^t(\nu\mathbf{k})u_{l'}(E_{\nu\mathbf{k}},R)Y_{m'}^{l'}(\tilde{\mathbf{R}}), \quad (7)$$

where the expansion coefficients $D_{l'm'}^t(\nu\mathbf{k})$ are determined by the boundary conditions on the sphere's surface. The component of $|\nu\mathbf{k}\rangle$ inside of sphere t is a coherent superposition of angular momentum eigenstates, which are defined with respect to a certain coordinate system centered on the atom.

From Eq. (7) we may derive the $l'm'$-like charge density inside of the atomic sphere t due to the band state $|\nu\mathbf{k}\rangle$,

$$\rho_{\nu\mathbf{k},l'm'}^t(\mathbf{R})=|D_{l'm'}^t(\nu\mathbf{k})u_{l'}(E_{\nu\mathbf{k}},R)Y_{m'}^{l'}(\tilde{\mathbf{R}})|^2. \quad (8)$$

Hence, by integration over the whole sphere t [by definition, $\int_0^{R_t}dRR^2|u_{l'}(R)|^2=1$], the local partial charge is

$$q_{\nu k,l'm'}^t=|D_{l'm'}^t(\nu k)|^2. \quad (9)$$

Summing all local partial charges of different band states but the same energy ϵ', we obtain the local partial DOS

$$\chi_{l'm'}^t(\epsilon')=\sum_{\nu\mathbf{k}}|D_{l'm'}^t(\nu\mathbf{k})|^2\delta(\epsilon'-E_{\nu\mathbf{k}}). \quad (10)$$

We use the expression Eq. (7) for the final states in the DFF Eq. (2), for the initial states we employ Eq. (5), and we insert the expansion Eq. (6) for the interaction operator. As stated above, the sum over i is a sum over the two spin orientations and the magnetic quantum number m, and we sum all transition probabilities to energetically allowed band states $|\nu\mathbf{k}\rangle$, taking care of the coherent expansion in Eq. (7) when calculating the modulus squared. In a way similar to the derivations in Refs. 4 and 5, transforming integrals over spherical harmonics into $3j$ symbols,[22] and defining the radial integrals

$$\langle j_\lambda(Q)\rangle_{n\epsilon'll'}=\int_0^{R_t}dR\,R^2\,u_{nl}(R)j_\lambda(QR)u_{l'}(\epsilon',R), \quad (11)$$

where $\epsilon'=E_{nl}+E$, we arrive at our main result

$$\begin{aligned}S(\mathbf{Q},E)=&2\sum_{l'm'}\sum_{L'M'}\sum_{\lambda\mu}\sum_{\lambda'\mu'}4\pi(-1)^{l'+L'}i^{\lambda-\lambda'}\\&\times(2l+1)\sqrt{(2\lambda+1)(2\lambda'+1)(2l'+1)(2L'+1)}\\&\times Y_\mu^\lambda(\tilde{\mathbf{Q}})^*Y_\mu^{\lambda'}(\tilde{\mathbf{Q}})\langle j_\lambda(Q)\rangle_{n\epsilon'll'}\langle j_{\lambda'}(Q)\rangle_{n\epsilon'lL'}\\&\times\begin{pmatrix}l&\lambda&l'\\0&0&0\end{pmatrix}\begin{pmatrix}l&\lambda'&L'\\0&0&0\end{pmatrix}\\&\times\sum_m\begin{pmatrix}l&\lambda&l'\\-m&\mu&m'\end{pmatrix}\begin{pmatrix}l&\lambda'&L'\\-m&\mu'&M'\end{pmatrix}\\&\times\sum_{\nu\mathbf{k}}D_{l'm'}^t(\nu\mathbf{k})D_{L'M'}^t(\nu\mathbf{k})^*\delta(\epsilon'-E_{\nu\mathbf{k}}).\end{aligned} \quad (12)$$

The factor 2 stems from the two spin orientations, and the $3j$ symbols express the tensorial character of $\exp(i\mathbf{QR})$, which

projects the final state on selected angular momenta l',L' and directions m',M'. This corresponds to the projection expressed by any scalar product **QR**. In case of small Q, all radial integrals in Eq. (11) with $\lambda \neq 1$ are small compared to the $(\lambda=1)$ contribution,[4] and then the first two $3j$ symbols represent the dipole-selection rule $l'=l\pm1, L'=l\pm1$. Therefore ELNES is said to test the dipole-selected local partial (i.e., l'-projected) DOS.

Surprisingly, the energy restricted sum over band states in the last line of Eq. (12) is *not* the local partial DOS defined in Eq. (10). Collecting all the terms preceding the energy-restricted sum in Eq. (12) into momentum- and energy-dependent coefficients, we may write, using the Kronecker symbols $c_{l'L'}$ and $\delta_{m'M'}$,

$$S(\mathbf{Q},E)=\sum_{l'm'} b_{l'm'}(\mathbf{Q},\epsilon')\chi^t_{l'm'}(\epsilon') + \sum_{l',L'}\sum_{m',M'} c_{l'L'm'M'}(\mathbf{Q},\epsilon')(1-\delta_{l'L'}\delta_{m'M'}) \times\sum_{\nu\mathbf{k}} D^t_{l'm'}(\nu\mathbf{k})D^t_{L'M'}(\nu\mathbf{k})^*\delta(\epsilon'-E_{\nu\mathbf{k}}). \quad (13)$$

The DFF is composed of one term proportional to the momentum- and direction-projected local DOS, and a second term containing contributions from the coupling of different final angular momenta, resulting from the coherent composition of the band state $|\nu\mathbf{k}\rangle$. These cross terms in Eq. (13) can be attributed to the fact that a special direction **Q** is selected in a nonspherically symmetric geometry, as was in fact already pointed out by Saldin.[23]

If we average Eq. (12) over all possible directions of **Q**, we obtain

$$\overline{S}_{[4\pi]}(Q,E)=\frac{1}{4\pi}\int_{[4\pi]} d^2\tilde{\mathbf{Q}}S(\mathbf{Q},E) =2(2l+1)\sum_{l'=0}^{\infty}\sum_{\lambda=|l-l'|}^{l+l'}(2\lambda+1) \times\begin{pmatrix} l & \lambda & l' \\ 0 & 0 & 0\end{pmatrix}^2 |\langle j_\lambda(Q)\rangle_{n\epsilon' ll'}|^2\chi^t_{l'}(\epsilon'). \quad (14)$$

In the step from Eq. (12) to Eq. (14) we made use of the orthogonality of the spherical harmonics and of

$$\sum_{m\mu}\begin{pmatrix} l & \lambda & l' \\ -m & \mu & m'\end{pmatrix}\begin{pmatrix} l & \lambda & L' \\ -m & \mu & M'\end{pmatrix}=\frac{\delta_{l'L'}\delta_{m'M'}}{2l'+1}. \quad (15)$$

Proceeding as in the step from Eq. (12) to Eq. (13),

$$\overline{S}_{[4\pi]}(Q,E)=\sum_{l'} a_{l'}(Q,\epsilon')\chi^t_{l'}(\epsilon'), \quad (16)$$

i.e., DFF and thus inelastic scattering cross section are indeed proportional to the local partial DOS

$$\chi^t_{l'}(\epsilon')=\sum_{m'=-l'}^{l'}\chi^t_{l'm'}(\epsilon'). \quad (17)$$

The coefficient $a_{l'}(Q,\epsilon')$ in Eq. (16) can be interpreted as the matrix element of Eq. (3). For small Q, it includes the dipole-selection rule, Eq. (4). Obviously, all cross terms in Eqs. (12) and (13) vanish as soon as we do not distinguish a particular direction, and this is what is done in the derivations of, e.g., Müller and Wilkins,[19] who correctly interpret x-ray absorption near-edge structure (XANES) spectra in terms of the partial DOS.

The — slightly nonchalant — reference to Fermi's golden rule as a ''derivation'' of Eq. (3), however, is wrong: multiplication of the transition-matrix element by the number of states per energy implies that transitions take place between eigenstates to the unperturbed Hamiltonian, and that the number of such eigenstates is counted. Eigenstates in a crystal are Bloch waves, labeled by $(\nu,\mathbf{k})$, and not angular momentum eigenstates, labeled by (l',m'). We implicitly applied Fermi's golden rule in summing over final band states $|\nu\mathbf{k}\rangle$ in Eq. (2). The coherent composition of each singular band state by angular momentum eigenstates gave rise to the cross terms of Eqs. (12) and (13).

III. DISCUSSION: *K*-SHELL EXCITATION TREATED IN THE DIPOLE APPROXIMATION

In the case of *K*-shell excitation treated in the dipole approximation, we have $l=0$, $m=0$ and $\lambda=\lambda'=1$. Equation (12) then simplifies to

$$S(\mathbf{Q},E)=2\sum_{\mu\mu'} 4\pi\cdot9\cdot Y^1_\mu(\tilde{\mathbf{Q}})^*Y^1_{\mu'}(\tilde{\mathbf{Q}}) \times\langle j_1(Q)\rangle^2_{n\epsilon'01}\begin{pmatrix} 0 & 1 & 1 \\ 0 & 0 & 0\end{pmatrix}^2\begin{pmatrix} 0 & 1 & 1 \\ 0 & \mu & -\mu\end{pmatrix} \times\begin{pmatrix} 0 & 1 & 1 \\ 0 & \mu' & -\mu'\end{pmatrix}\sum_{\nu\mathbf{k}} D^t_{1,-\mu}(\nu\mathbf{k}) \times D^t_{1,-\mu'}(\nu\mathbf{k})^*\delta(\epsilon'-E_{\nu\mathbf{k}}), \quad (18)$$

where we made use of the properties of the $3j$ symbols imposing $l'=L'=1$ and $m'=-\mu, M'=-\mu'$ for nonvanishing $S(\mathbf{Q},E)$. Using explicit formulas for the $3j$ symbols[22] and the definition of the generalized local p-DOS

$$\Xi^t_{p,\mu,\mu'}(\epsilon')=\sum_{\nu\mathbf{k}} D^t_{1,\mu}(\nu\mathbf{k})D^t_{1,\mu'}(\nu\mathbf{k})^*\delta(\epsilon'-E_{\nu\mathbf{k}}), \quad (19)$$

Eq. (18) transforms into

$$S(\mathbf{Q},E)=8\pi\sum_{\mu\mu'} Y^1_\mu(\tilde{\mathbf{Q}})^*Y^1_{\mu'}(\tilde{\mathbf{Q}})\langle j_1(Q)\rangle^2_{n\epsilon'01}(-1)^{\mu+\mu'} \times\Xi^t_{p,-\mu,-\mu'}(\epsilon')=:\sum_{\mu\mu'} S_{\mu\mu'}(\mathbf{Q},E). \quad (20)$$

A. Interpretation in the (l',m') basis

Interpretation of Eq. (20) is straightforward: In the momentum-resolved experiment we project the final state on the direction of $\mathbf{Q}$, therefore we select certain μ,μ' components of the final state that are linked to the orientation of $\mathbf{Q}$ in the chosen coordinate system (in which the μ,μ' components of the final state are defined) via the spherical harmonics with argument $\tilde{\mathbf{Q}}$. Expression (20) considers such projection on single components of the final state in terms with $\mu=\mu'$, which relate to the dipole-allowed local p-DOS

$$\chi^t_{p,\mu}(\epsilon')=\Xi^t_{p,\mu,\mu}(\epsilon'), \tag{21}$$

but it also accounts for the coherence of the final-state wave function by simultaneous projection on μ and μ' components with $\mu'\neq\mu$. The latter contribution to the DFF we call the cross-term contribution, and in the special case of *K*-shell excitation treated in the dipole approximation this cross-term contribution follows from Eq. (20) by summation over $\mu,\mu'=-1,0,+1$, keeping only summands with $\mu\neq\mu'$. The sum contains six terms, and remarking that for each $S_{\mu\mu'}(\mathbf{Q},E)$ in Eq. (20) the relation $S_{\mu\mu'}(\mathbf{Q},E)=S_{\mu'\mu}(\mathbf{Q},E)^*$ holds (this is necessary in order to obtain real quantities for the DFF), we may write

$$S_{\mathrm{CT}_{m'}}(\mathbf{Q},E)=2\,\mathrm{Re}[S_{+1,-1}(\mathbf{Q},E)+S_{0,+1}(\mathbf{Q},E)+S_{0,-1}(\mathbf{Q},E)], \tag{22}$$

whereas the contribution to the DFF directly proportional to the m'-like DOS reads

$$S_{\mathrm{DOS}_{m'}}(\mathbf{Q},E)=8\pi\langle j_1(Q)\rangle^2_{n\epsilon'01}\sum_\mu |Y^1_\mu(\tilde{\mathbf{Q}})|^2\chi^t_{p,-\mu}(\epsilon'). \tag{23}$$

B. Treatment using p_x,p_y,p_z orbitals

The DFF is composed by one part proportional to the m'-like p-character DOS, Eq. (23), and a second part containing the cross terms from simultaneous occupation of different m' orbitals, Eq. (22). However, it is often desirable and more clear to identify contributions due to''chemical'' p_x, p_y, and p_z orbitals aligned parallel to the x, y, and z axes, respectively. These are defined by

$$\begin{aligned} p_x(\tilde{\mathbf{R}}) &:= -\frac{1}{\sqrt{2}}[Y^1_{+1}(\tilde{\mathbf{R}})-Y^1_{-1}(\tilde{\mathbf{R}})]=\sqrt{\frac{3}{4\pi}}\frac{R_x}{R},\\ p_y(\tilde{\mathbf{R}}) &:= +\frac{i}{\sqrt{2}}[Y^1_{+1}(\tilde{\mathbf{R}})+Y^1_{-1}(\tilde{\mathbf{R}})]=\sqrt{\frac{3}{4\pi}}\frac{R_y}{R},\\ p_z(\tilde{\mathbf{R}}) &:= Y^1_0(\tilde{\mathbf{R}})=\sqrt{\frac{3}{4\pi}}\frac{R_z}{R}. \end{aligned} \tag{24}$$

The inversion of Eq. (24) is

$$\begin{aligned} Y^1_{\pm1}(\tilde{\mathbf{R}}) &= \mp\frac{1}{\sqrt{2}}[p_x(\tilde{\mathbf{R}})\pm ip_y(\tilde{\mathbf{R}})],\\ Y^1_0(\tilde{\mathbf{R}}) &= p_z(\tilde{\mathbf{R}}). \end{aligned} \tag{25}$$

With these relations we expand the p component of band state $|\nu\mathbf{k}\rangle$ Eq. (7) inside of the atomic sphere t in terms of orbital functions,

$$\psi^t_{\nu\mathbf{k},p}(\mathbf{R})=[D^t_x(\nu\mathbf{k})p_x(\tilde{\mathbf{R}})+D^t_y(\nu\mathbf{k})p_y(\tilde{\mathbf{R}})+D^t_z(\nu\mathbf{k})p_z(\tilde{\mathbf{R}})]u_{l'=1}(E_{\nu\mathbf{k}},R) \tag{26}$$

with

$$\begin{aligned} D^t_x(\nu\mathbf{k}) &:= -\frac{1}{\sqrt{2}}[D^t_{1,+1}(\nu\mathbf{k})-D^t_{1,-1}(\nu\mathbf{k})],\\ D^t_y(\nu\mathbf{k}) &:= -\frac{i}{\sqrt{2}}[D^t_{1,+1}(\nu\mathbf{k})+D^t_{1,-1}(\nu\mathbf{k})],\\ D^t_z(\nu\mathbf{k}) &:= D^t_{1,0}(\nu\mathbf{k}), \end{aligned} \tag{27}$$

or, inversely,

$$\begin{aligned} D^t_{1,\pm1}(\nu\mathbf{k}) &= \mp\frac{1}{\sqrt{2}}[D^t_x(\nu\mathbf{k})\mp iD^t_y(\nu\mathbf{k})],\\ D^t_{1,0}(\nu\mathbf{k}) &= D^t_z(\nu\mathbf{k}). \end{aligned} \tag{28}$$

The p_x,p_y,p_z character DOS is defined as $\chi^t_{p_x,p_y,p_z}(\epsilon')=\Sigma_{\nu\mathbf{k}}|D^t_{x,y,z}(\nu\mathbf{k})|^2\delta(\epsilon'-E_{\nu\mathbf{k}})$, respectively, and in the appendix the relations between the various x,y,z, and $+1,0,-1$ p-character DOS are discussed. Making use of Eq. (25) and Eqs. (A1) and (A4) derived in the appendix, we translate the DFF in m' representation into x,y,z representation. The contribution proportional to the m'-like p-character DOS, Eq. (23), reads

$$S_{\mathrm{DOS}_{m'}}(\mathbf{Q},E)=3\langle j_1(Q)\rangle^2_{n\epsilon'01}\left\{\frac{Q_x^2+Q_y^2}{Q^2}[\chi^t_{p_x}(\epsilon')+\chi^t_{p_y}(\epsilon')]+2\frac{Q_z^2}{Q^2}\chi^t_{p_z}(\epsilon')\right\}, \tag{29}$$

whereas the cross-term contribution Eq. (22) is the sum of

$$\begin{aligned} &2\,\mathrm{Re}[S_{+1,-1}(\mathbf{Q},E)]\\ &=\langle j_1(Q)\rangle^2_{n\epsilon'01}\left\{3\frac{Q_x^2-Q_y^2}{Q^2}[\chi^t_{p_x}(\epsilon')-\chi^t_{p_y}(\epsilon')]+12\frac{Q_xQ_y}{Q^2}\sum_{\nu\mathbf{k}}\mathrm{Re}[D^t_x(\nu\mathbf{k})D^t_y(\nu\mathbf{k})^*]\delta(\epsilon'-E_{\nu\mathbf{k}})\right\} \end{aligned} \tag{30}$$

and

$$2\,\mathrm{Re}[S_{0,+1}(\mathbf{Q},E)+S_{0,-1}(\mathbf{Q},E)]$$

$$=\frac{12\langle j_1(Q)\rangle^2_{n\epsilon' 01}}{Q^2}$$

$$\times\Bigg\{-Q_zQ_x\sum_{\nu\mathbf{k}}\mathrm{Re}[D^t_z(\nu\mathbf{k})D^t_x(\nu\mathbf{k})^*]\delta(\epsilon'-E_{\nu\mathbf{k}})$$

$$-Q_zQ_y\sum_{\nu\mathbf{k}}\mathrm{Re}[D^t_z(\nu\mathbf{k})D^t_y(\nu\mathbf{k})^*]$$

$$\times\delta(\epsilon'-E_{\nu\mathbf{k}})\Bigg\}. \tag{31}$$

We see that part of the $-1,+1$ cross term may in fact be interpreted by a pure p_x,p_y DOS contribution, which is due to p_x and p_y orbitals being a combination of $(1,-1)$ and $(1,+1)$ states.

An interpretation of the DFF in terms of p_x, p_y, and p_z orbitals yields a term proportional to the p_x, p_y, or p_z like DOS

$$S_{\mathrm{DOS}_{xyz}}(\mathbf{Q},E)=\frac{6\langle j_1(Q)\rangle^2_{n\epsilon' 01}}{Q^2}[Q_x^2\chi^t_{p_x}(\epsilon')+Q_y^2\chi^t_{p_y}(\epsilon')$$

$$+Q_z^2\chi^t_{p_z}(\epsilon')], \tag{32}$$

and a second term proportional to cross products of expansion coefficients into p_x, p_y, or p_z orbitals,

$$S_{\mathrm{CT}_{xyz}}(\mathbf{Q},E)=\frac{12\langle j_1(Q)\rangle^2_{n\epsilon' 01}}{Q^2}$$

$$\times\Bigg\{+Q_xQ_y\sum_{\nu\mathbf{k}}\mathrm{Re}[D^t_x(\nu\mathbf{k})D^t_y(\nu\mathbf{k})^*]$$

$$\times\delta(\epsilon'-E_{\nu\mathbf{k}})-Q_zQ_x\sum_{\nu\mathbf{k}}$$

$$\times\mathrm{Re}[D^t_z(\nu\mathbf{k})D^t_x(\nu\mathbf{k})^*]\delta(\epsilon'-E_{\nu\mathbf{k}})$$

$$-Q_zQ_y\sum_{\nu\mathbf{k}}\mathrm{Re}[D^t_z(\nu\mathbf{k})D^t_y(\nu\mathbf{k})^*]$$

$$\times\delta(\epsilon'-E_{\nu\mathbf{k}})\Bigg\}. \tag{33}$$

C. Existence of cross terms

The genuine coherence terms in Eq. (33) represent the symmetry of the final state. Only if the local point-group symmetry permits choice of a coordinate system with equivalence of negative and positive axes for at least one of the directions coupled, i.e., if the plane perpendicular to that direction is a mirror plane, these coherences disappear. Indeed, imagine the (yz) plane to be a mirror plane, $+x$ equivalent to $-x$. Then the physics of the problem do not change whether we employ a scattering vector (Q_x,Q_y,Q_z) or a scattering vector $(-Q_x,Q_y,Q_z)$. In other words, the sum of Eqs. (32) and (33), $S(\mathbf{Q},E)=S_{\mathrm{DOS}_{xyz}}(\mathbf{Q},E)+S_{\mathrm{CT}_{xyz}}(\mathbf{Q},E)$, must be the same in the two cases. Equation (32) is independent of the sign of Q_x, but the Q_x-dependent lines of Eq. (33) change sign when the mirror is applied to $\mathbf{Q}$. As we demand identity of the two DFF for any values of Q_y,Q_z, both sums over $(\nu,\mathbf{k})$, which are multiplied by Q_x must vanish.

The disappearance of the cross terms corresponds to the diagonalization of the photoelectron's density matrix, where the p_x,p_y, and p_z orbitals in that special coordinate system become eigenstates of the photoelectron. In cases, where the respective site has a point group symmetry with at least two perpendicular mirror planes (i.e., at least for two of the three axes the positive and negative directions are equivalent) it is in principle always possible to choose a coordinate system such that cross terms can be avoided. However, with lower symmetry this is not possible for a general $\mathbf{Q}$ direction.

In $(l'm')$ representation, the same argument applies for the $S_{0,+1}(\mathbf{Q},E),S_{0,-1}(\mathbf{Q},E)$ cross terms. The $S_{-1,+1}(\mathbf{Q},E)$ term, however, disappears only if additionally to two perpendicular mirror planes, the x and the y axis are equivalent. This can again be shown by a symmetry argument for $\mathbf{Q}$, similar to that of the preceding paragraph and applied to the $(Q_x^2-Q_y^2)$ term in Eq. (30). More obviously, equivalence of x and y axis implies $\chi^t_{p_x}(\epsilon')=\chi^t_{p_y}(\epsilon')$. Then, Eq. (A3) is valid and the first part of the cross-term contribution Eq. (30) disappears. Such complete annulment of the $S_{-1,+1}(\mathbf{Q},E)$ term can only be achieved for symmetries higher than orthorhombic.

As a general remark, it must be stated that a $\mathbf{Q}$-resolved ELNES (or an $\boldsymbol{\epsilon}$-resolved XANES) experiment tests one single direction onto which the electron states are projected. It is, therefore, always possible to exclude all cross term and (xy)-plane DOS contributions, when the coordinate system is chosen such that $\mathbf{Q}$ is aligned to the z axis, $Q_x=Q_y=0$. From Eq. (32) we see that in this case the DFF is directly proportional to the local p_z DOS and all cross-terms in Eq. (33) or Eq. (22) are zero. Once the coordinate system is chosen, anisotropy of the atomic environment [e.g., $\chi^t_{p_x}(\epsilon')\neq\chi^t_{p_z}(\epsilon')$] will result in anisotropy of the obtained spectra when $\mathbf{Q}$ is tilted off the z axis, according to Eq. (32). Such experiments are reported in, e.g., Refs. 7 and 13. Additional evidence for a dependence of the signal on the sign of the components Q_x,Q_y,Q_z is traced back to the cross-term contribution according to Eq. (33) and accounts for antisymmetry of the atomic environment projected on the x, y, and z axis.

IV. EXAMPLE: OXYGEN K-SHELL EXCITATION IN RUTILE

From a practical point of view, the $(l'm')$ basis is much easier to use than Cartesian orbital functions, especially when going beyond the dipole approximation and when shells other than the K shell are studied. We therefore implemented[24] Eq. (12) in the LAPW (linearized augmented plane waves) code WIEN97 (Ref. 25). The question how to find the LAPW equivalent of $D^t_{l'm'}(\nu\mathbf{k})D^t_{l'm'}(\nu\mathbf{k})^*$ and other numerical details shall be treated elsewhere.[26] Here, we just present the simulation of the ELNES due to K-shell excitation $(n=1,l=0)$ of one particular oxygen atom in rutile

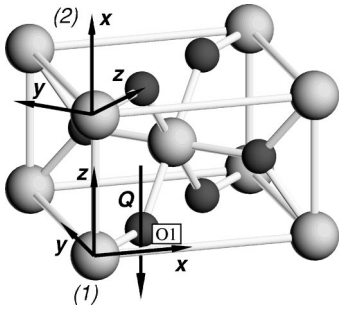

FIG. 1. Unit cell of TiO_2 (rutile). For simulation of the ELNES the two coordinate systems (1) and (2) were used.

TiO_2, labeled by O1 in Fig. 1. The electronic structure and chemical bonding in TiO2 was studied in detail in Ref. 27. We choose for Q two different orientations with respect to the crystal, one in [001] direction (parallel to the c axis, see Fig. 1) and one along the [110] direction, keeping the absolute length constant at $Q=3.9\ \mathrm{nm}^{-1}$ (this corresponds to the minimum length of Q due to an energy loss of 530 eV at 200 keV primary energy). Calculations are performed using two different coordinate systems (1) and (2). In order to show the relation between DOS and spectrum more clearly, we did not include instrumental and life-time broadening in the simulations. In the chosen example, $Q \ll a_K^{-1}$ with a_K the approximate extension of the oxygen K shell, so that the dipole selection rule applies. Consequently, cross terms couple different m', M' of p-character final states ($l'=L'=1$), and we may refer to the results of discussion in the preceding section.

Figure 2 gives the ELNES of O1 with **Q** parallel to the c axis of tetragonal rutile according to Eq. (23) where just the symmetry-projected DOS is used. This yields the correct result only in coordinate system (1) where **Q** is aligned to the z axis and cross terms as well as in-plane DOS contributions disappear. There, the result is directly proportional to the p_z-like DOS $\chi^t_{p_z}(\epsilon')$ shown in Fig. 3. In the second coordinate system, which is actually the one used by the band-structure code, **Q** is parallel to the x axis. However, the result is not proportional to the p_x-like DOS [which is of course identical to the p_z-like DOS of coordinate system (1), cf. Figs. 3 and 4] because the calculation is based on the (l',m') representation, and there the cross terms of Eq. (22) must be taken into account. The correction that is necessary in order to obtain the same result as in coordinate system (1) is given by the first part of Eq. (30), proportional to the difference of p_x- and p_y-like DOS defined with respect to coordinate system (2). Indeed, we must not expect any genuine cross terms described in Eq. (33) when using the coordinate system (2) since both (110) and (001) planes are mirror planes for the local environment of O1, i.e., $+x$ and $-x$ as well as $+y$ and

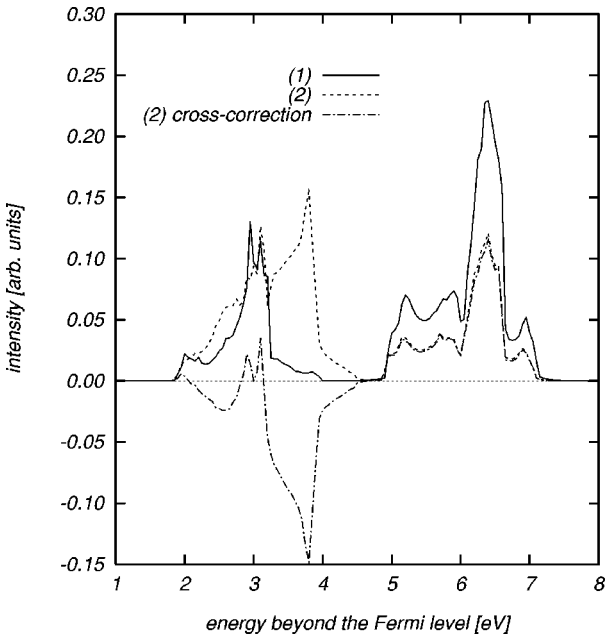

FIG. 2. Simulation of the ELNES due to K-shell excitation of the oxygen atom O1 in Fig. 1 with **Q** in [001] direction. The solid line corresponds to the DOS-based formula Eq. (23) using coordinate system (1), where it yields the correct result for the given **Q**. The dashed line is the result of Eq. (23) in coordinate system (2). The dash-dotted line is the cross-term correction necessary in system (2), proportional to $\chi^t_{p_x}(\epsilon')-\chi^t_{p_y}(\epsilon')$.

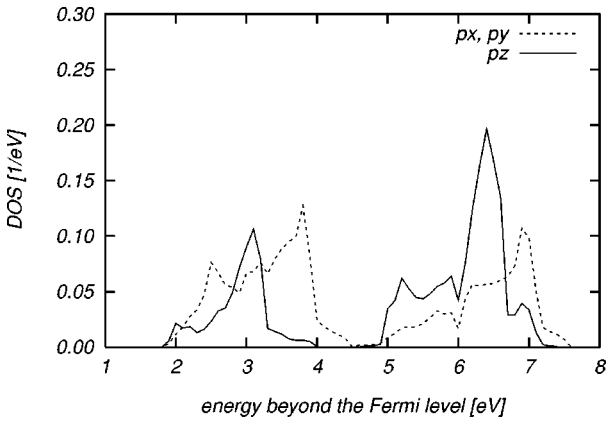

FIG. 3. Local p-character DOS beyond the Fermi level of oxygen, defined in system (1). Due to the (110) mirror, $\chi^t_{p_x}(\epsilon')=\chi^t_{p_y}(\epsilon')$. The spectrum obtained with **Q** parallel to [001] is proportional to $\chi^t_{p_z}(\epsilon')$, cf. Fig. 2.

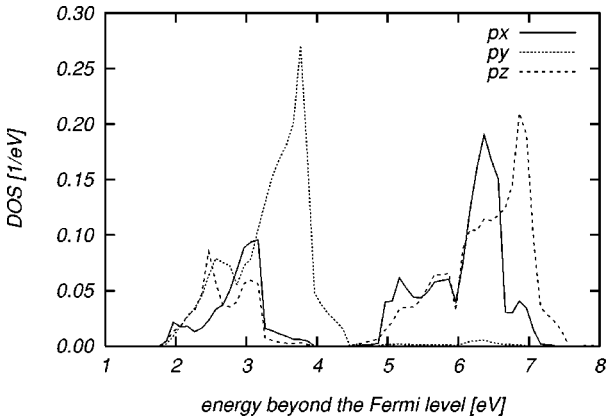

FIG. 4. Same as Fig. 3, but defined in system (2). All three components of the DOS are different, the p_x-like DOS is identical to the p_z-like DOS defined in coordinate system (1). A spectrum obtained with **Q** parallel to the [110] direction will be proportional to $\chi^t_{p_z}(\epsilon')$, cf. Fig. 5.

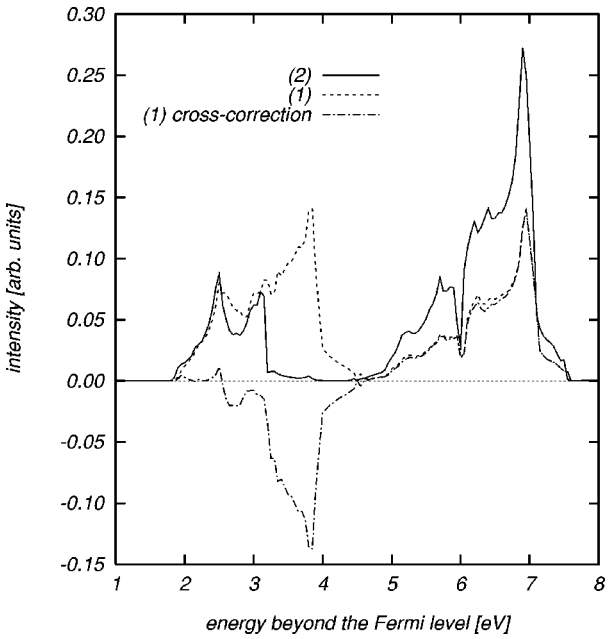

FIG. 5. Simulation of the ELNES due to *K*-shell excitation of the oxygen atom O1 in Fig. 1 with **Q** parallel to the [110] direction in tetragonal rutile. The solid line is the true spectrum, which for the given **Q** and using coordinate system (2), results from the DOS-based formula Eq. (23). The dashed line is the result of Eq. (23) using coordinate system (1). In this system, and with **Q** pointing in [110] direction, the cross-term correction is necessary (dash-dotted line). In contrast to Fig. 2, this cross term cannot be traced back to a difference of DOS components, but is caused by the xy-coupling term in Eq. (33).

$-y$ are equivalent. The mere inequivalence of $+z$ and $-z$ [the lacking mirror (110)] is insufficient to create zx- or zy-coupling cross-terms. Note that the cross-term correction in the Ti-t_{2g} band[27] (the energy region between 2 and 4.5 eV beyond the Fermi level) has (mostly) opposite sign than the contribution of the $(l'm')$-DOS based formula Eq. (23), while in the Ti-e_g band (from 5 to 7 eV) sign and magnitude coincide. This is a consequence of the required nonzero overlap between the respective O-p_x and p_y orbitals with the Ti-d orbitals of e_g or t_{2g} symmetry, respectively. This is also the reason, why the p_y DOS in coordinate system (2) is almost zero in the Ti-e_g band.

The situation is different with **Q** parallel to the [110] direction, where the resulting spectrum is shown as solid line in Fig. 5. The spectrum is directly proportional to the p_z-like DOS if coordinate system (2) is used, as may be seen by comparing Figs. 4 and 5, and therefore may be described by Eq. (23) alone. Using coordinate system (1), neither $+x$, $-x$ nor $+y,-y$ directions are equivalent, and we obtain genuine xy-coupling cross terms of the type described in Eq. (33). Since the x and y axis of coordinate system (1) are equivalent [due to the mirror (110)], $\chi^t_{p_x}(\epsilon')=\chi^t_{p_y}(\epsilon')$ and the $(+1,-1)$ cross term of Eq. (30) is always identical to the xy-coupling cross term. Nevertheless, in the Ti-e_g band the cross-term correction is again of equal sign and magnitude as the $(l'm')$-DOS contribution.

V. CONCLUSION

We have derived a formula that permits correct quantitative simulation of momentum-resolved ELNES or polarization-dependent XANES experiments within band-structure methods in reciprocal space. The interest of such experiments is the possibility to study the detailed geometry and partition of unoccupied electronic states, and this in turn implies the interpretation of spectra in terms of the local symmetry-projected DOS. The theoretically and numerically simplest approach is based on a (l',m') representation of the unoccupied states. For local point-group symmetries lower than orthorhombic, an interpretation in terms of just the (l',m') DOS is insufficient, and coupling of different momenta of the final state must be considered. As was discussed for the special case of the *K*-shell excitation treated in the dipole approximation, such cross terms may partly be traced back to DOS contributions in a Cartesian coordinate system. If, however, the local point-group symmetry does not contain at least two mirror planes perpendicular to each other, cross terms will persist even in a Cartesian picture, and an interpretation using only the DOS is impossible. This in turn makes **Q**-dependent ELNES experiments sensitive to not just differences of the unoccupied states along orthogonal directions, but also to inversion symmetry along one single direction. Thus it is hoped that the presented approach stimulates both theoreticians and experimentalists to continue studies in this prospering field.

ACKNOWLEDGMENTS

We thank C. Blaas and E. Balcar for helpful discussions. M.N. acknowledges support of the European Union under TMR Contract No. ERBFM-BICT961416.

APPENDIX A: RELATIONS BETWEEN THE DOS

For the local p-character DOS we derive from Eq. (28)

$$\chi^t_{p,-1}(\epsilon')=\frac{1}{2}[\chi^t_{p_x}(\epsilon')+\chi^t_{p_y}(\epsilon')]+\sum_{\nu\mathbf{k}}\mathrm{Im}[D^t_x(\nu\mathbf{k})D^t_y(\nu\mathbf{k})^*]\delta(\epsilon'-E_{\nu\mathbf{k}}),$$

$$\chi^t_{p,+1}(\epsilon')=\frac{1}{2}[\chi^t_{p_x}(\epsilon')+\chi^t_{p_y}(\epsilon')]-\sum_{\nu\mathbf{k}}\mathrm{Im}[D^t_x(\nu\mathbf{k})D^t_y(\nu\mathbf{k})^*]\delta(\epsilon'-E_{\nu\mathbf{k}}),$$

$$\chi^t_{p,0}(\epsilon')=\chi^t_{p_z}(\epsilon') \tag{A1}$$

and from Eq. (27)

$$\chi^t_{p_x}(\epsilon') := \sum_{\nu\mathbf{k}} |D^t_x(\nu\mathbf{k})|^2 \delta(\epsilon' - E_{\nu\mathbf{k}}) = \tfrac{1}{2}[\chi^t_{p_{+1}}(\epsilon') + \chi^t_{p_{-1}}(\epsilon')] - \mathrm{Re}[\Xi^t_{p,+1,-1}(\epsilon')], \tag{A2}$$

$$\chi^t_{p_y}(\epsilon') := \sum_{\nu\mathbf{k}} |D^t_y(\nu\mathbf{k})|^2 \delta(\epsilon' - E_{\nu\mathbf{k}}) = \tfrac{1}{2}[\chi^t_{p_{+1}}(\epsilon') + \chi^t_{p_{-1}}(\epsilon')] + \mathrm{Re}[\Xi^t_{p,+1,-1}(\epsilon')],$$

$$\chi^t_{p_z}(\epsilon') := \sum_{\nu\mathbf{k}} |D^t_z(\nu\mathbf{k})|^2 \delta(\epsilon' - E_{\nu\mathbf{k}}) = \chi^t_{p,0}(\epsilon').$$

If we can choose a system of coordinates such that x and y axis become equivalent,

$$\chi^t_{p_x}(\epsilon') \equiv \chi^t_{p_y}(\epsilon') \Rightarrow \mathrm{Re}[\Xi^t_{p,+1,-1}(\epsilon')] = 0. \tag{A3}$$

This is also seen in the generalized expressions

$$\Xi^t_{p,-1,+1}(\epsilon') = -\tfrac{1}{2}[\chi^t_{p_x}(\epsilon') - \chi^t_{p_y}(\epsilon')] - i\sum_{\nu\mathbf{k}} \mathrm{Re}[D^t_x(\nu\mathbf{k}) D^t_y(\nu\mathbf{k})^*]\delta(\epsilon' - E_{\nu\mathbf{k}}), \tag{A4}$$

$$\Xi^t_{p,0,-1}(\epsilon') = +\frac{1}{\sqrt{2}} \sum_{\nu\mathbf{k}} D^t_z(\nu\mathbf{k})[D^t_x(\nu\mathbf{k})^* - iD^t_y(\nu\mathbf{k})^*] \times \delta(\epsilon' - E_{\nu\mathbf{k}}),$$

$$\Xi^t_{p,0,+1}(\epsilon') = -\frac{1}{\sqrt{2}} \sum_{\nu\mathbf{k}} D^t_z(\nu\mathbf{k})[D^t_x(\nu\mathbf{k})^* + iD^t_y(\nu\mathbf{k})^*] \times \delta(\epsilon' - E_{\nu\mathbf{k}}).$$

[1] M. Inokuti, Rev. Mod. Phys. **43**, 297 (1971).
[2] J. Fink, N. Nücker, E. Pellegrin, H. Romberg, M. Alexander, and M. Knupfer, J. Electron Spectrosc. Relat. Phenom. **66**, 395 (1996).
[3] D. A. Muller, D. J. Singh, and J. Silcox, Phys. Rev. B **57**, 8181 (1998).
[4] S. T. Manson, Phys. Rev. A **6**, 1013 (1972).
[5] R. D. Leapman, P. Rez, and D. Mayers, J. Chem. Phys. **72**, 1232 (1980).
[6] G. A. Botton, G. Y. Guo, W. M. Temmerman, and C. J. Humphreys, Phys. Rev. B **54**, 1682 (1996).
[7] K. Lie, R. Holmestad, K. Marthinsen, and R. Høier, Phys. Rev. B **57**, 1585 (1998).
[8] C. Colliex and B. Jouffrey, Philos. Mag. **25**, 491 (1972).
[9] O. L. Krivanek, M. M. Disko, J. Taftø, and J. C. H. Spence, Ultramicroscopy **9**, 249 (1982).
[10] P. Rez, J. Bruley, P. Brohan, M. Payne, and L. A. J. Garvie, Ultramicroscopy **59**, 159 (1995).
[11] *Unoccupied Electronic States*, edited by J. C. Fuggle and J. E. Inglesfield (Springer, Berlin, 1992).
[12] G. A. Botton, C. B. Boothroyd, and W. M. Stobbs, Ultramicroscopy **59**, 93 (1995).
[13] R. D. Leapman, P. L. Fejes, and J. Silcox, Phys. Rev. B **28**, 2361 (1983).
[14] P. J. Durham, J. B. Pendry, and C. H. Hodges, Comput. Phys. Commun. **25**, 193 (1982).
[15] D. D. Vvedensky, D. K. Saldin, and J. B. Pendry, Comput. Phys. Commun. **40**, 421 (1986).
[16] X. Weng and P. Rez, Phys. Rev. B **39**, 7405 (1989).
[17] R. Brydson, J. Phys. D **29**, 1699 (1996).
[18] P. Rez, in *Transmission Electron Energy Loss Spectrometry in Materials Science*, edited by M. M. Disko, C. C. Ahn, and B. Fultz (The Minerals, Metals & Materials Society, Warrendale, PA, 1992), Chap. 5.
[19] J. E. Müller and J. W. Wilkins, Phys. Rev. B **29**, 4331 (1984).
[20] A. Neckel, K. Schwarz, R. Eibler, P. Rastl, and P. Weinberger, Mikrochim. Acta Suppl. **6**, 257 (1975).
[21] J. C. Slater, Phys. Rev. **51**, 846 (1937).
[22] L. D. Landau and E. M. Lifshitz, *Quantum Mechanics, Non-relativistic Theory*, 3rd ed. (Pergamon Press, Oxford, 1977).
[23] D. K. Saldin, Philos. Mag. B **56**, 515 (1987).
[24] The program shall be included in the next release of WIEN97.
[25] P. Blaha, K. Schwarz, and J. Luitz, WIEN97 (Vienna University of Technology, 1997). [Updated Unix version of P. Blaha, K. Schwarz, P. Sorantin, and S. B. Trickey, Comput. Phys. Commun. 59, 399 (1990)].
[26] P.-H. Louf, C. Hebert-Souche, P. Blaha, M. Nelhiebel, J. Luitz, P. Schattschneider, K. Schwarz, and B. Jouffrey (unpublished).
[27] P. I. Sorantin and K. Schwarz, Inorg. Chem. **31**, 567 (1992).